Available online at www.sciencedirect.com

SciVerse ScienceDirect

Ceramics International 39 (2013) 7211–7215

CERAMICS INTERNATIONAL

www.elsevier.com/locate/ceramint

Strong green light emission in Ho doped $Bi_4Ti_3O_{12}$ ferroelectric ceramics

T. Wei[a,*], Q.J. Zhou[a], C.Z. Zhao[b], Y.B. Lin[c], Y.L. Zou[a], Y. Li[a], L.S. Zhang[a]

[a]College of Science, Civil Aviation University of China, Tianjin 300300, China
[b]School of Electronics and Information Engineering, Tianjin Polytechnics University, Tianjin 300160, China
[c]Institute for Advanced Materials, South China Academy of Advanced Photonics Engineering, South China Normal University, Guangzhou 510006, China

Received 2 February 2013; received in revised form 19 February 2013; accepted 19 February 2013
Available online 27 February 2013

Abstract

A series of polycrystalline $Bi_{4-x}Ho_xTi_3O_{12}$ (BiT:xHo^{3+}) ($x=0.0$, 0.01, 0.03, 0.05, 0.1, 0.15, 0.2, 0.3, and 0.4) samples were synthesized through the solid-state reaction method, and their microstructural, photoluminescence, ferroelectric (FE), and dielectric properties were investigated. Under the excitation of 455 nm light, the sample exhibits a strong green emission peak centered at 545 nm which corresponds to the transition from $^5S_2$ to $^5I_8$. The optimal emission intensity was obtained when $x=0.05$ for the BiT:xHo^{3+} system. More importantly, enhanced ferroelectric and dielectric properties were also obtained with Ho doping.
© 2013 Elsevier Ltd and Techna Group S.r.l. All rights reserved.

Keywords: C. Dielectric properties; X-ray diffraction; Photoluminescence; Ferroelectricity

1. Introduction

Bismuth layer-structured ferroelectrics (BLSFs), a group of important and interesting ferroelectrics, have been investigated extensively for the applications of piezoelectric, ferroelectric, dielectric, pyroelectric, electrooptic, photocatalytic, and biosensing fields owing to their multifunctional characteristics [1–6]. BLSFs are defined as $Bi_2A_{n-1}B_nO_{3n+3}$, where A is a large 12-coordinate cation, B is a small 6-coordinate cation, and n represents the number of BO_6 octahedron. The crystal structure of BLSFs is described as an alternate stacking of the Bi_2O_2 layer and pseudo-perovskite layers along the c axis.

Among the BLSFs, ferroelectric bismuth titanate ($Bi_4Ti_3O_{12}$(BiT)) has great potential for the application in electro-optic devices field because BiT shows a low deposition temperature and a large spontaneous polarization (P_S) [7,8]. Currently, mixed $Bi_{4-x}Re_xTi_3O_{12}$ (BRTx), where Re is the rare earth element, is attractive to researchers because of its excellent and rich physics relative to pure BiT [1,7–11]. Park et al. reported that La^{3+} doping at the Bi^{3+} site can greatly improve the ferroelectric properties of BiT [1]. Furthermore, Chon et al. reported that the Nd-modified bismuth titanate (BNdT) system exhibits remarkable ferroelectric properties in which the switchable remanent polarization is about 100 μC/cm^2 and no imprinting or fatigue behavior is detected [7]. It is understood that these Re^{3+} ion substitutions at Bi^{3+} site can enhance the stability of TiO_6 octahedra against oxygen vacancies, thus resulting the excellent ferroelectric properties of the BRTx system.

On the other hand, photoluminescence properties of the rare earth doped BLSFs have attracted much attention for possible integrated photoluminescent ferroelectric device applications. Recent reports reveal that the relatively low-level Re^{3+} (such as Pr^{3+}, Ce^{3+}, Nd^{3+}, Sm^{3+}, Eu^{3+}, Dy^{3+}, and Er^{3+} ions) doping at the Bi^{3+} site can greatly improve the photoluminescence properties of BLSFs [12–17]. Among these material systems, layered perovskite-type BiT doped with Re^{3+} (for example, Eu, Er, Pr, Nd etc.) has attracted renewed interests due to its excellent photoluminescence properties. However, to our best knowledge, the photoluminescence properties of Ho^{3+} ions doped BiT are still missing. Considering that Ho^{3+} is an important activator ion of inorganic photoluminescent materials, it is

*Corresponding author. Tel.: +86 15122848807; fax: +86 022 24092514.
E-mail address: weitong.nju@gmail.com (T. Wei).

0272-8842/$ - see front matter © 2013 Elsevier Ltd and Techna Group S.r.l. All rights reserved.
http://dx.doi.org/10.1016/j.ceramint.2013.02.067

of interest and significance to study photoluminescence properties of the Ho^{3+} doped BiT system.

In this work, Ho^{3+} doped BiT (BiT:xHo^{3+}) ceramics with different concentrations were synthesized through the solid state reaction method. The photoluminescence properties of the ceramics were firstly reported. Strong green emission excited by blue light has been successfully observed at room temperature. Furthermore, the ferroelectric and dielectric properties were also investigated for the BiT:xHo^{3+} system. As a multifunctional material, it is believed that BiT:xHo^{3+} may be useful in light-emitting diode, sensor and optical-electrointegration.

2. Experimental procedures

The polycrystalline $Bi_{4-x}Ho_xTi_3O_{12}$ (BiT:xHo^{3+}) (x= 0.0, 0.01, 0.03, 0.05, 0.1, 0.15, 0.2, 0.3, and 0.4) ceramics were synthesized by the conventional solid-state reaction [18,19]. Highly purified powders Bi_2O_3 (99%), Ho_2O_3 (99%), and TiO_2 (99.99%) were weighed to prepare BiT:xHo^{3+} samples. Bi_2O_3 was 3% excess in the starting powder to compensate for the Bi vaporization during the thermal annealing. After mixing by milling in alcohol for 24 h using agate pots and agate balls in a planetary mill, the as-prepared powders were dried and then calcined at 850 °C for 5 h. The resultant powders were reground and pelletized under 15 MPa pressure into disks of 13 mm in diameter and sintered at 1150 °C for 2 h.

The phase analysis and crystal structures of the prepared BiT:xHo^{3+} samples were evaluated using X-ray diffraction (XRD) (DX-2000 diffractometer) at room temperature. The photoluminescence (PL) spectra at room temperature were recorded by using a Jobin Yvon HR320 fluorescence spectrophotometer. Gold electrodes were sputtered on sample surfaces for electrical measurements. The ferroelectric (FE) behaviors were measured with a Radiant Precision Multiferroic Tester (Radiant Technologies Ltd., Albuquerque, NM) in a standard mode. The dielectric permittivity (ε_r) and loss factor ($\tan\delta$) as a function of frequency were measured using an Agilent E4980 Precision LCR Meter.

3. Results and discussions

Fig. 1 shows the XRD patterns of BiT:xHo^{3+} samples with x ranging from 0.0 to 0.4. All of the diffraction peaks can be indexed according to the standard diffraction pattern data of BiT and agree well with the Joint Committee for Powder Diffraction Standards Card (No. 65-2527). No other non-bismuth layered structure phases, such as Ho_2O_3, Bi_2O_3, and TiO_2, are detected in the current XRD pattern. It implies that the Ho^{3+} ions have entered into the pseudo-perovskite unit cell maintaining the Bi-layered Aurivillius structure of the solid solution.

Compared with the pure BiT orthorhombic phase, obvious shifts are observed in the peak positions for the BiT:xHo^{3+} samples. Amplification of the (200) diffraction peak is also presented in Fig. 1. One can see that the (200) diffraction peak shifts to high angle side with the increase of Ho^{3+} ions concentration. Referring to the ion radius of Ho^{3+} (1.015 Å, CN8) and Bi^{3+} (1.170 Å, CN8) [20], remarkable lattice distortion associated with the doping of Ho^{3+} at Bi^{3+} site can be introduced in the BiT:xHo^{3+} system.

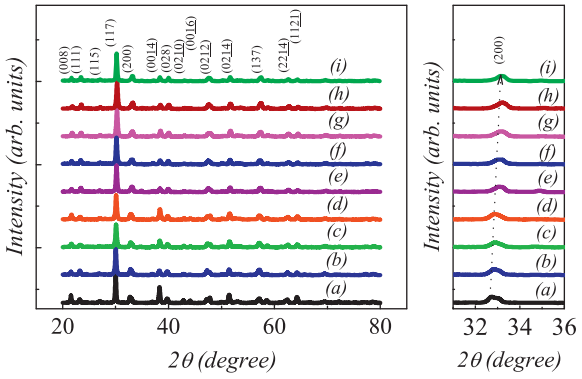

Fig. 1. XRD pattern of the BiT:xHo^{3+} system with different Ho^{3+}-doped concentrations: (a) x=0.0, (b) x=0.01, (c) x=0.03, (d) x=0.05, (e) x=0.1, (f) x=0.15, (g) x=0.2, (h) x=0.3, and (i) x=0.4.

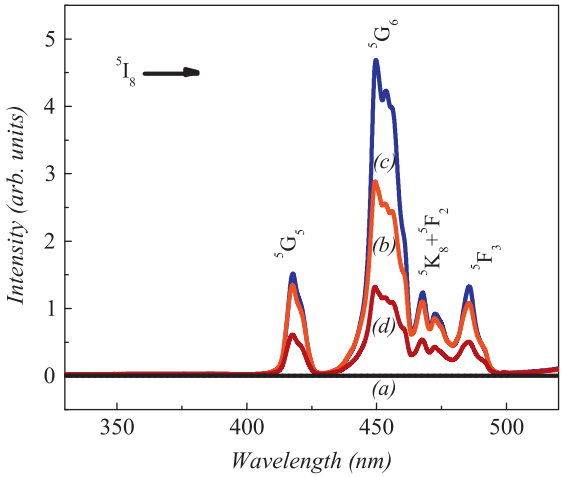

Fig. 2. Photoluminescence excitation (PLE) spectra monitored at 545 nm of BiT:xHo^{3+} with x=0.0 (a), 0.03 (b), 0.05 (c), and 0.3 (d).

Now we focus on the photoluminescence properties of the BiT:xHo^{3+} system. To understand the excitation paths of Ho^{3+} ions, Fig. 2 gives the photoluminescence excitation (PLE) spectra associated with different Ho^{3+} concentrations of BiT:xHo^{3+} samples by monitoring the 545 nm emission at room temperature. Clearly, strong sharp excitation peaks between 410 and 500 nm can be clearly detected which correspond to the f–f transitions from the $^5I_8$ ground state to the excited states of Ho^{3+} [21–23]. The excitation peak around 418 nm is attributed to the $^5I_8 \rightarrow {}^5G_5$ transition. The remarkably sharp excitation peak around 455 nm corresponded to the $^5I_8 \rightarrow {}^5G_6$ transition. Furthermore, the excitation peak around 468 nm and 472 nm can be

attributed to the $^5I_8 \rightarrow {}^5K_8$ and $^5I_8 \rightarrow {}^5F_2$ transitions, respectively. In addition, the excitation peak around 485 nm should correspond to the $^5I_8 \rightarrow {}^5F_3$ transition. No shifts of the excited peaks for all of the BiT:xHo^{3+} samples are observed. What is interesting is that the remarkable excitation band locates around the emission wavelength of commercial blue light-emitting diodes (LEDs) (450–470 nm) which indicates BiT:xHo^{3+} can act as a potential blue light exciting phosphor [24,25].

Fig. 3 displays the photoluminescence (PL) spectra of BiT:xHo^{3+} samples with different Ho^{3+} ions concentrations excited at 455 nm at room temperature. Under the resonant excitation at 455 nm, the broad bands peaking around 545 nm, 657 nm, and 753 nm owing to intra f–f transition of Ho^{3+} ions are obtained. In order to clearly illustrate the photoluminescence process, the simplified energy level diagram is given in Fig. 4. Under the 455 nm light excitation, electrons can be excited to the $^5G_6$ level. The excited electrons can non-radiatively relax to the $^5S_2$ state and recombine to the lower level of $^5I_8$ which gives the strong green emission as shown in Figs. 3 and 4 [21–23]. The weak red emission centered at 656 nm corresponds to the $^5F_5 \rightarrow {}^5I_8$ transition. In addition, the weak 753 nm emission peak is due to the $^5I_4 \rightarrow {}^5I_8$ transition.

Furthermore, from Figs. 2 and 3, one can see that the excitation and emission intensities for BiT:xHo^{3+} samples are tightly related with the Ho^{3+} doping concentration. The dependence of the excitation (e.g. the $^5I_8 \rightarrow {}^5G_6$ excitation peak) and emission (e.g. the $^5S_2 \rightarrow {}^5I_8$ emission peak) intensities on Ho^{3+} concentration is presented in Fig. 5. With the increasing Ho^{3+} concentration, it can be seen that both the excitation and emission intensities first increase and reach their maximum when $x=0.05$. Then, with x further increasing, the excitation and emission intensities start to decrease due to the concentration quenching effect [26,27]. It is known that when the doping concentration reaches a certain degree, the distance between Ho^{3+} ions became small and a fraction

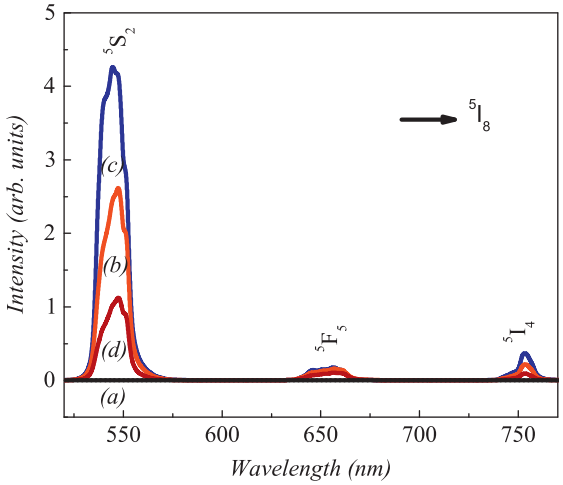

Fig. 3. Photoluminescence (PL) spectra of BiT:xHo^{3+} samples with $x=0.0$ (a), 0.03 (b), 0.05 (c), and 0.3 (d), excited at 455 nm.

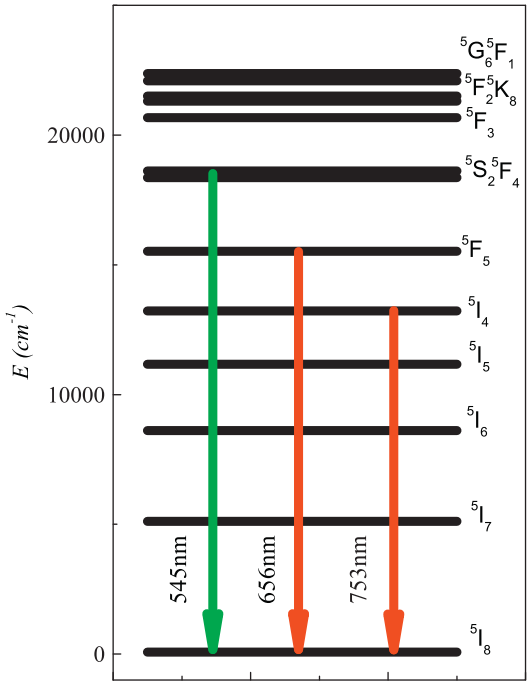

Fig. 4. Energy level scheme of Ho^{3+}. The solid arrows indicate the 545 nm, 657 nm, and 753 nm luminescence.

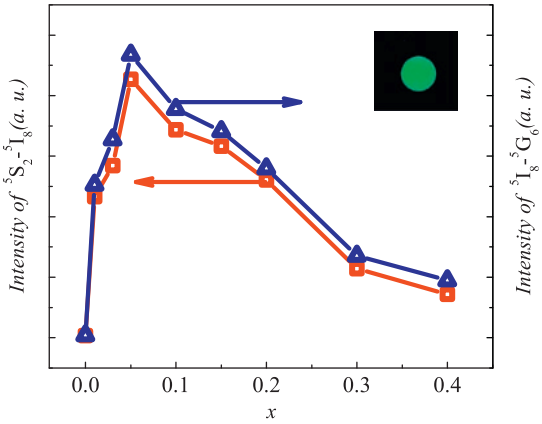

Fig. 5. Variations of the excitation and emission intensities versus x. The inset of the figure gives a luminescence photograph of $x=0.05$.

of energy migrated to the quenchers. From the above results, BiT:xHo^{3+} with $x=0.05$ sample exhibits optimized photoluminescence. In addition, the inset of Fig. 5 gives a luminescence photograph of $x=0.05$ obtained in darkness by a common digital camera under the excitation of a blue commercial LED (3 W, 460–470 nm). Strong green emission was clearly observed by naked eyes at room temperature.

Besides the excellent blue excited green emission feature, BiT:xHo^{3+} is also an important ferroelectric material. Thus, to confirm the multifunctional properties of BiT:xHo^{3+}, ferroelectric measurement was also carried out at room temperature. Referring to the optimized photoluminescence of BiT:xHo^{3+} with $x=0.05$, Fig. 6 representatively shows the measured typical polarization–electric field (P–E) hysteresis

[28,29] loops of $x=0.0$ and $x=0.05$ clearly. It can be seen that the remanent polarization $2P_r$ of $x=0.05$ is about 16 μC/cm^2, which is higher than that of $x=0.0$ ($2P_r \sim 11$ μC/cm^2). The improved ferroelectric behavior can be attributed to the Ho^{3+} doping. The possible origin of the improvement of $2P_r$ for $x=0.05$ should be contributed to the enhanced stability of TiO_6 octahedra, thus resulting the improved ferroelectric properties [1,7–11].

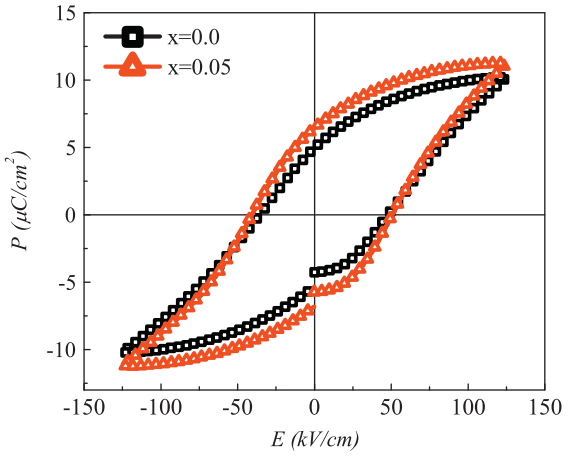

Fig. 6. *P–E* hysteresis loops at room temperature for $x=0.0$ and 0.05.

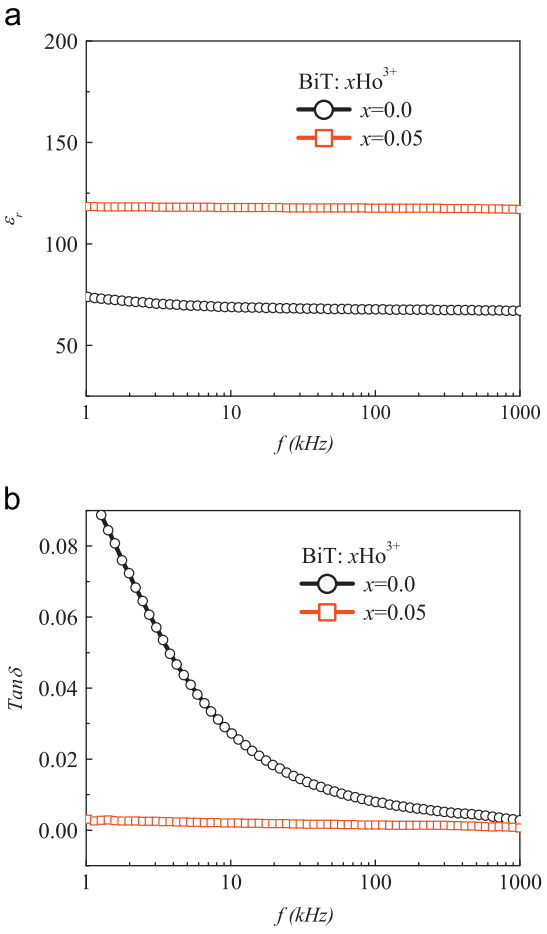

Fig. 7. Variation of dielectric permittivity (ε_r) and loss factor (tan δ) with frequency for $x=0.0$ and 0.05.

Finally, the enhanced electrical properties of BiT:xHo^{3+} with $x=0.05$ are also demonstrated through dielectric properties measurement by using an Agilent E4980 Precision LCR Meter. Fig. 7(a) presents the variation of dielectric permittivity (ε_r) and loss factor (tan δ) with frequency for these two samples: $x=0.0$ and $x=0.05$. It can be seen that ε_r for $x=0.05$ is about twice over that of $x=0.0$ sample. The ε_r for $x=0.05$ reaches up to 118, however, the tan δ as given in Fig. 7(b) is only 0.002 at 10 kHz which is much lower than that of $x=0.0$ (e.g. the tan δ is about 0.027 at 10 kHz). The enhanced ε_r and low tan δ should be ascribed to the Ho^{3+} doping in BiT which improves the stability of lattice and decreases the defects, for example, oxygen vacancies, and bismuth vacancies.

4. Conclusion

In conclusion, BiT:xHo^{3+} ceramics were synthesized by the traditional solid state method. The photoluminescence properties of the BiT:xHo^{3+} samples were investigated. An intense green emission band centered at around 545 nm is observed which is due to the transition from $^5S_2$ to $^5I_8$. The excitation bands are mainly located at 410–500 nm, which are adaptable to the emission band of commercial blue light-emitting diodes (LEDs) chips. The optimal emission intensity was obtained when $x=0.05$ for the BiT:xHo^{3+} system. More importantly, BiT:xHo^{3+} with $x=0.05$ also possesses enhanced ferroelectric and dielectric properties. So, as a type of multifunctional material, BiT:xHo^{3+} with $x=0.05$ system may play an important role in many fields such as light-emitting diode, sensor, and optical-electrointegration.

Acknowledgment

This work was supported by the Natural Science Foundation of China (51102277, 51002183, and 61079010), and the Fundamental Research Funds for the Central Universities (ZXH2012P008, ZXH2012K006, and ZXH2012D016).

References

[1] B.H. Park, B.S. Kang, S.D. Bu, T.W. Noh, J. Lee, W. Jo, Lanthanum-substituted bismuth titanate for use in non-volatile memories, Nature 401 (1999) 682–684.
[2] P. de Araujo, C.A. Cuchiaro, J.D. McMillan, L.D.M.C. Scott, J.F. Scott, Fatigue free ferroelectric capacitors with platinum electrodes, Nature 374 (1995) 627–629.
[3] M.D. Maeder, D. Damjanovic, N. Setier, Lead free piezoelectric materials, Journal of Electroceramics 13 (2004) 385–392.
[4] Y.X. Li, G. Chen, H.J. Zhang, Z.H. Li, J.X. Sun, Electronic structure and photocatalytic properties of $ABi_2Ta_2O_9$ (A=Ca, Sr, Ba), Journal of Solid State Chemistry 181 (2008) 2653–2659.
[5] J.Q. Hu, Y. Yu, H. Guo, Z.W. Chen, A.Q. Li, X.M. Feng, B.M. Xi, G.Q. Hu, Sol–gel hydrothermal synthesis and enhanced biosensing

properties of nanoplated lanthanum-substituted bismuth titanate microspheres, Journal of Materials Chemistry 21 (2011) 5352–5359.
[6] Z.J. Zhang, W.Z. Wang, W.Z. Yin, M. Shang, L. Wang, S.M. Sun, Inducing photocatalysis by visible light beyond the absorption edge: effect of upconversion agent on the photocatalytic activity of Bi_2WO_6, Applied Catalysis B 101 (1–2) (2010) 68–73.
[7] U. Chon, H.M. Jang, M.G. Kim, C.H. Chang, Layered perovskites with giant spontaneous polarizations for nonvolatile memories, Physical Review Letters 89 (2002) 087601–087604.
[8] H.N. Lee, D. Hesse, N. Zakharov, U. Gosele, Ferroelectric $Bi_{3.25}La_{0.75}Ti_3O_{12}$ films of uniform *a*-axis orientation on silicon substrates, Science 296 (2002) 2006–2009.
[9] R.E. Melgarejo, M.S. Tomar, S. Bhaskar, P.S. Dobal, R.S. Katiyar, Large ferroelectric response in $Bi_{4-x}Nd_xTi_3O_{12}$ films prepared by sol–gel process, Applied Physics Letters 81 (2002) 2611.
[10] Z.X. Cheng, C.V. Kannan, K. Ozawa, H. Kimura, X.L. Wang, Orientation dependent ferroelectric properties in samarium doped bismuth titanate thin films grown by the pulsed-laser-ablation method, Applied Physics Letters 89 (2006) 032901.
[11] X.J. Zheng, L. He, Y.C. Zhou, M.H. Tang, Effects of europium content on the microstructural and ferroelectric properties of $Bi_{4-x}Eu_xTi_3O_{12}$ thin films, Applied Physics Letters 89 (2006) 252908.
[12] M.E. Villafuerte-Castrejón, F. Camacho-Alanís, F. Gonźalez, A. Ibarra-Palos, G. Gonźalez, L. Fuentes, L. Bucio, Luminescence and structural study of $Bi_{4-x}Eu_xTi_3O_{12}$ solid solution, Journal of the European Ceramic Society 27 (2007) 545–549.
[13] K.B. Ruan, X.M. Chen, T. Liang, G.H. Wu, D.H. Bao, Improved photoluminescence and electrical properties of Eu- and Gd-codoped bismuth titanate ferroelectric thin films, Journal of Applied Physics 103 (2008) 086104.
[14] H. Zhou, G.H. Wu, N. Qin, D.H. Bao, Dual enhancement of photoluminescence and ferroelectric polarization in Pr^{3+}/La^{3+}-codoped bismuth titanate thin films, Journal of the American Ceramic Society 93 (2010) 2109–2112.
[15] K. Aizawa, Y. Ohtani, Ferroelectric and luminescent properties of Eu-doped $SrBi_2Ta_2O_9$ films, Japanese Journal of Applied Physics 46 (1) (2007) 6944–6947.
[16] K.Y. Ko, Y.K. Lee, Y.R. Do, Y.D. Huh, Structural effect of a two-dimensional SiO_2 photonic crystal layer on extraction efficiency in sputter-deposited $Y_2O_3:Eu^{3+}$ thin-film phosphors, Journal of Applied Physics, 102 (2007) 013509.
[17] D.F. Peng, X.S. Wang, C.N. Xu, X. Yao, J. Lin, T.T. Sun, Bright upconversion emission, increased Tc, enhanced ferroelectric and piezoelectric properties in Er-doped $CaBi_4Ti_4O_{15}$ multifunctional ferroelectric oxides, Journal of the American Ceramic Society 96 (2013) 184–190.
[18] T. Wei, J.-M. Liu, Q.J. Zhou, Q.G. Song, Coupling and competition between ferroelectric and antiferroelectric states in Ca-doped $Sr_{0.9-x}Ba_{0.1}Ca_xTiO_3$: multipolar states, Physical Review B 83 (2011) 052101.
[19] T. Wei, Q.G. Song, Q.J. Zhou, Z.P. Li, Y.F. Chen, X.L. Qi, S.Q. Guo, J.-M. Liu, Giant dielectric tunable behavior of Pr-doped $SrTiO_3$ at low temperature, Functional Materials Letters 5 (2012) 1250018.
[20] R.D. Shannon, Revised effective ionic radii and systematic studies of interatomie distances in halides and chaleogenides, Acta Crystallographica A 32 (1976) 751–767.
[21] W.T. Camall, P.R. Fields, K. Rajnak, Spectral intensities of the trivalent lanthanides and actinides in solution II. Pm^{3+}, Sm^{3+}, Eu^{3+}, Gd^{3+}, Tb^{3+}, Dy^{3+}, and Ho^3, Journal of Chemical Physics 49 (1968) 4412–4423.
[22] V.R. Bandi, B.K. Grandhe, M. Jayasimhadri, K. Jang, H.S. Lee, S.S. Yi, J.H. Jeong, Photoluminescence and structural properties of $Ca_3Y(VO_4)_3$ RE^{3+} (=Sm^{3+}, Ho^{3+} and Tm^{3+}) powder phosphors for tri-colors, Journal of Crystal Growth 326 (2011) 120–123.
[23] G.J. Ding, F. Gao, G.H. Wu, D.H. Bao, Bright up-conversion green photoluminescence in Ho^{3+}–Yb^{3+} co-doped $Bi_4Ti_3O_{12}$ ferroelectric thin films, Journal of Applied Physics 109 (2011) 123101.
[24] S. Nakamura, G. Fasol, The Blue Laser Diode: GaN Based Light Emitters and Lasers, Springer, Berlin, 1997.
[25] H.Q. Sun, D.F. Peng, X.S. Wang, M.M. Tang, Q.W. Zhang, X. Yao, Strong red emission in Pr doped $(Bi_{0.5}Na_{0.5})TiO_3$ ferroelectric ceramics, Journal of Applied Physics 110 (2011) 016102.
[26] R. Naik, N. Karanjikar, M. Razvi, Concentration quenching of fluorescence from $^1D_2$ state of Pr^{3+} in YPO_4, Journal of Luminescence 54 (1992) 139–144.
[27] H. Chen, R. Lian, M. Yin, L. Lou, W. Zhang, S. Xia, J. Krupa, Luminescence concentration quenching of $^1D_2$ state in $YPO_4:Pr^{3+}$, Journal of Physics: Condensed Matter 13 (2001) 1151–1158.
[28] T. Wei, C. Zhu, K.F. Wang, H.L. Cai, J.S. Zhu, J.-M. Liu, Influence of A-site codoping on ferroelectricity of quantum paraelectric $SrTiO_3$, Journal of Applied Physics 103 (2008) 124104.
[29] T. Wei, Q.J. Zhou, X. Yang, Q.G. Song, Z.P. Li, X.L. Qi, J.-M. Liu, Competition between quantum fluctuation and ferroelectric order in $Eu_{1-x}Ba_xTiO_3$, Applied Surface Science 258 (2012) 4601–4606.